An Implicit Gradient Meshfree Formulation for Convection-Dominated Problems

M. Hillman and J.S. Chen

Abstract Meshfree approximations are ideal for the gradient-type stabilized Petrov–Galerkin methods used for solving Eulerian conservation laws due to their ability to achieve arbitrary smoothness, however, the gradient terms are computationally demanding for meshfree methods. To address this issue, a stabilization technique that avoids high order differentiation of meshfree shape functions is introduced by employing implicit gradients under the reproducing kernel approximation framework. The modification to the standard approximation introduces virtually no additional computational cost, and its implementation is simple. The effectiveness of the proposed method is demonstrated in several benchmark problems.

1 Introduction

While Galerkin methods have proven successful in a variety of problems, the application of standard versions of these methods can yield disastrous results for non-self-adjoint problems, such as the Eulerian descriptions of conservation laws with strong convection. In particular, when boundary layers are present, these methods yield large oscillations that destroy the solution. A class of stabilized Petrov–Galerkin methods [1–3] has been developed that provide stable solutions for these problems.

Stabilized methods have been analyzed mathematically [2–4], can be justified by the variational multiscale framework [5, 6], and can be constructed by static condensation of bubble functions [7–9]. In these methods, portions of the differential operator, or the entire operator, are included in the test function. The streamline upwind Petrov–Galerkin (SU/PG) method [1] was motivated by performing

M. Hillman • J.S. Chen (✉)
Department of Structural Engineering, University of California, San Diego, 9500 Gilman Drive, La Jolla, CA 92093-0085, USA
e-mail: js-chen@ucsd.edu

Y. Bazilevs, K. Takizawa (eds.), *Advances in Computational Fluid-Structure Interaction and Flow Simulation*, Modeling and Simulation in Science, Engineering and Technology, DOI 10.1007/978-3-319-40827-9_3

stabilization in a consistent and streamline manner, and also put to rest notions of artificial diffusion. The Galerkin/least squares (G/LS) method [2] gave a more general framework to achieve stability by employing a weighted least squares of the residual. The subgrid scale (SGS) method gave improved stability for higher order elements [3] and reaction-dominated problems [7].

Though originally developed for finite elements, these approaches have been applied to meshfree methods as well. The reproducing kernel particle method (RKPM) with the standard stabilization approach has been applied to flow problems [10]. Suitable stabilization parameters for meshfree methods have been discussed [11], and stabilized meshfree and finite element coupled schemes have also been proposed [12] to achieve a combination of the computational efficiency of finite elements with the flexibility of handling difficult topological changes of the domain such as moving obstacles. A higher order accurate time integration scheme [13] has also been developed for meshfree methods for convection-dominated problems. Although the higher order derivatives involved in the gradient-type stabilization techniques can be calculated straightforwardly by taking advantage of the arbitrary smoothness in the meshfree approximation functions, they are computationally demanding.

The issue of computational efficiency of meshfree methods with gradient-type stabilization for convection-dominated problems is the cost of constructing derivatives of meshfree approximations. One remedy is to introduce implicit gradients [14], which originated from the synchronized convergence approximation [15, 16], where the completeness properties of approximation derivatives are imposed directly. Implicit gradients have been utilized for easing the computational cost of meshfree collocation methods [14], which require higher order derivatives. Implicit gradients have also been used to achieve gradient-type regularization for strain localization problems [17] and avoid the issue of boundary conditions associated with these methods.

In this work, the implicit gradient reproducing kernel particle method (IG-RKPM) is introduced for convection-dominated problems. A gradient reproducing condition is employed to construct the stabilizing gradient terms. This allows three standard stabilization techniques to be performed under a unified framework without the explicit computation of higher order derivatives of the shape functions. The proposed technique is computationally efficient, and it also simplifies stabilization procedures.

The remainder of this text is organized as follows. Section 2 reviews the numerical difficulties associated with convection-dominated problems, and common methods for stabilization. The implicit gradient reproducing kernel particle method is then introduced in Section 3, and the selection of a suitable stabilization parameter for meshfree methods is discussed. Several benchmark problems are solved in Section 4 to demonstrate the effectiveness of the proposed method. Concluding remarks are then given in Section 5.

2 Stabilization for Convection-Dominated Problems

2.1 Advection–Diffusion Equation

The advection–diffusion equation is considered herein as a model problem for convection-dominated problems. The strong form asks to find u such that

$$\begin{aligned} \mathcal{L}u &= s \quad \text{in } \Omega \\ u &= g \quad \text{on } \partial\Omega_g \\ \mathcal{B}u &= h \quad \text{on } \partial\Omega_h \end{aligned} \tag{1}$$

where s is a source term, $\partial\Omega_g$ and $\partial\Omega_h$ are the essential and natural boundaries of the domain, respectively, the flux boundary conditions $\mathcal{B}u = k\nabla u \cdot \mathbf{n}$ are considered herein, and the operator $\mathscr{L}$ in (1) is

$$\mathcal{L}u = -\nabla \cdot (\mathbf{K} \cdot \nabla u - \mathbf{a}u) \tag{2}$$

where $\mathbf{a}$ is the advection velocity and $\mathbf{K}$ is the diffusivity tensor. Without loss of generality, we consider a divergence-free advection field and the case of isotropic diffusion with $\mathbf{K} = \mathbf{I}k$, where $\mathbf{I}$ is the identity tensor, and k is a constant scalar, for which $\mathcal{L}u = -\left(k\nabla^2 u - \mathbf{a} \cdot \nabla u\right)$.

The weak form of (1) is to find $u \in U$ such that

$$B(v,u) = L(v) \qquad \forall v \in V \tag{3}$$

where

$$B(v,u) = (k\nabla v, \nabla u)_\Omega + (v, \mathbf{a} \cdot \nabla u)_\Omega, \tag{4}$$

$$L(v) = (v,s)_\Omega + (v,h)_{\Gamma_h}. \tag{5}$$

Here $U = \left\{ u \in H^1(\Omega) \middle| \, u = g \text{ on } \Gamma_g \right\}$, $V = \left\{ v \in H^1(\Omega) \middle| \, v = 0 \text{ on } \Gamma_g \right\}$, and $(\cdot,\cdot)_\Omega$ and $(\cdot,\cdot)_{\Gamma_h}$ denote the L^2 inner product on the domain and natural boundary, respectively. The Galerkin method for solving (3) is to find $u^h \in U^h$ that satisfies

$$B\left(v^h, u^h\right) = L\left(v^h\right), \qquad \forall v^h \in V^h \tag{6}$$

where $U^h \subset U$ and $V^h \subset V$ are suitable finite-dimensional subspaces.

For discrete solutions of the advection–diffusion equation with grid dimension or node spacing h, the critical value defining how the numerical solution will behave is the grid Péclet number $Pe_h = \|\mathbf{a}\| h/2k$. When the grid Péclet number is greater than unity, standard Bubnov–Galerkin methods lose coercivity and become unstable, and the instability manifests as large oscillations in the presence of fine-scale features such as boundary layers which can appear in the solution of the model problem (1).

2.2 Stabilized Methods

The stabilized methods SU/PG, G/LS, and SGS can be phrased in terms of the Galerkin form of the original problem with a modified test function expressed in a unified fashion as:

$$\tilde{v}^h = v^h + \tau \mathbb{L} v^h \tag{7}$$

where τ is a stabilization parameter, and $\mathbb{L}$ is a differential operator that varies depending on the method:

$$\begin{array}{ll} \mathbb{L} = \mathcal{L}_{\text{adv}} & \text{SU/PG} \quad [1] \\ \mathbb{L} = \mathcal{L} & \text{G/LS} \quad [2] \\ \mathbb{L} = -\mathcal{L}^* & \text{SGS} \quad [3] \end{array} \tag{8}$$

In the above, $\mathscr{L}_{\text{adv}}$ is the advective portion of $\mathscr{L}$, and $\mathcal{L}^*$ is the adjoint of $\mathscr{L}$:

$$\mathcal{L}_{\text{adv}} = \mathbf{a} \cdot \nabla, \tag{9}$$

$$\mathcal{L}^* = -\left(k\nabla^2 + \mathbf{a} \cdot \nabla\right). \tag{10}$$

Stabilized methods are well justified [2–4], and can also be viewed as approximate variational multiscale methods [4, 6]. Stability estimates for SU/PG and SGS require invoking inverse estimates for the shape functions, while for G/LS stability follows directly. The stabilized form of the problem (6) can be stated as to find $u^h \in U^h \subset U$ such that

$$B\left(\tilde{v}^h, u^h\right) = L\left(\tilde{v}^h\right), \qquad \forall \tilde{v}^h \in V^h \tag{11}$$

where $V^h \subset V$, and U and V are adequate Sobolev spaces.

3 Implicit Gradient RKPM for Stabilization of Convection-Dominated Problems

3.1 Reproducing Kernel Approximation

The reproducing kernel (RK) approximation $u^h(\mathbf{x})$ of a function $u(\mathbf{x})$ is constructed by the product of a kernel function $\Phi_\rho(\mathbf{x} - \mathbf{x}_I)$ and a correction function [18, 19]:

$$\Psi_I(\mathbf{x}) = \mathbf{b}^{\mathrm{T}}(\mathbf{x})\, \mathbf{H}(\mathbf{x} - \mathbf{x}_I)\, \Phi_\rho(\mathbf{x} - \mathbf{x}_I) \tag{12}$$

where $\Psi_I(\mathbf{x})$ is the RK shape function, $\mathbf{H}(\mathbf{x}-\mathbf{x}_I) = \left[1\ x\ y\ x^2\ \ldots\ y^n\right]^{\mathrm{T}}$ is a column vector containing the complete n^{th} order monomials, and $\mathbf{b}^{\mathrm{T}}(\mathbf{x})$ is a row vector of coefficients to be determined. The correction function $\mathbf{b}^{\mathrm{T}}(\mathbf{x})\,\mathbf{H}(\mathbf{x}-\mathbf{x}_I)$ allows the approximation to reproduce any linear combination of monomials contained in $\mathbf{H}(\mathbf{x}-\mathbf{x}_I)$. The kernel function $\Phi_\rho(\mathbf{x}-\mathbf{x}_I)$ has compact support measure ρ, and the order of continuity of $\Phi_\rho(\mathbf{x}-\mathbf{x}_I)$ determines the continuity of $\Psi_I(\mathbf{x})$.

The coefficient vector $\mathbf{b}^{\mathrm{T}}(\mathbf{x})$ is obtained by enforcing the following reproducing conditions:

$$\sum_{I=1}^{NP} \Psi_I(\mathbf{x})\, x_{1I}^i x_{2I}^j = x_1^i x_2^j \quad 0 \le i+j \le n. \tag{13}$$

Substituting (12) into (13), the RK shape functions are constructed as

$$\Psi_I(\mathbf{x}) = \mathbf{H}(\mathbf{0})^{\mathrm{T}}\mathbf{M}(\mathbf{x})^{-1}\mathbf{H}(\mathbf{x}-\mathbf{x}_I)\,\Phi_\rho(\mathbf{x}-\mathbf{x}_I) \tag{14}$$

where

$$\mathbf{M}(\mathbf{x}) = \sum_{I=1}^{NP} \mathbf{H}(\mathbf{x}-\mathbf{x}_I)\,\mathbf{H}^{\mathrm{T}}(\mathbf{x}-\mathbf{x}_I)\,\Phi_\rho(\mathbf{x}-\mathbf{x}_I) \tag{15}$$

is called the moment matrix.

3.2 *Implicit Gradient Reproducing Kernel Particle Method*

The stabilization method SU/PG requires constructing second order derivatives of the approximation functions in (14), and for GL/S and SGS, third order derivatives are required, and construction of higher order derivatives of meshfree shape functions can be particularly expensive due to the need to take derivatives of $\mathbf{M}(\mathbf{x})^{-1}$. To avoid this computational expense, the implicit gradient reproducing kernel particle method is introduced. The basic idea is to achieve the same form of stabilized test functions (7) without explicit differentiation. To accomplish this, the following modification to the reproducing condition (13) is introduced for construction of the test functions:

$$\sum_{I=1}^{NP} \tilde{\Psi}_I^{\alpha}(\mathbf{x})\, x_{1I}^i x_{2I}^j = x_1^i x_2^j + \tau\mathbb{L}\left(x_1^i x_2^j\right), \quad 0 \le i+j \le n \tag{16}$$

where $\tilde{\Psi}_I^{\alpha}$ is the IG-RKPM shape function and $\mathbb{L}$ is the operator in (8). The reproducing condition (16) can be expressed in a generalized fashion as

$$\sum_{I=1}^{NP} \tilde{\Psi}_I^{\alpha}(\mathbf{x})\, x_{1I}^i x_{2I}^j = x_1^i x_2^j + \tau \sum_{i+j=0}^{n} \alpha_{ij} D_{ij}\left(x_1^i x_2^j\right), \quad 0 \le i+j \le n \tag{17}$$

where $D_{ij} = \partial^{i+j}/\partial x_1^i \partial x_2^j$ and the coefficients α_{ij} are determined based on the operator $\mathbb{L}$. The above can then be recast as [17]:

$$\sum_{I=1}^{NP} \tilde{\Psi}_I^{\alpha}(\mathbf{x})\,(x_1 - x_{1I})^i (x_2 - x_{2I})^j = \delta_{i0}\delta_{j0} + \tau\alpha_{ij}(-1)^{i+j} i!j!, \quad 0 \le i+j \le n. \tag{18}$$

Consider now the implicit gradient shape function in the following form:

$$\tilde{\Psi}_I^{\alpha}(\mathbf{x}) = \mathbf{b}_{\alpha}^{\mathrm{T}}(\mathbf{x})\,\mathbf{H}(\mathbf{x}-\mathbf{x}_I)\,\Phi_{\rho}(\mathbf{x}-\mathbf{x}_I) \tag{19}$$

where $\mathbf{b}_{\alpha}^{\mathrm{T}}(\mathbf{x})$ is a row vector of coefficients which satisfy (17). Following the same procedure as the previous sub-section, the coefficients $\mathbf{b}_{\alpha}^{\mathrm{T}}(\mathbf{x})$ can be obtained, resulting in the following construction for the implicit gradient approximation:

$$\tilde{\Psi}_I^{\alpha}(\mathbf{x}) = \mathbf{H}_{\alpha}^{\mathrm{T}}\mathbf{M}(\mathbf{x})^{-1}\mathbf{H}(\mathbf{x}-\mathbf{x}_I)\,\Phi_{\rho}(\mathbf{x}-\mathbf{x}_I) \tag{20}$$

where $\mathbf{H}_{\alpha}$ is a matrix containing terms from the right-hand side of (18). The values in this matrix are presented in Table 1.

Remark Comparing (20) to (14), it can be seen that the first term on the right-hand side of (20) is the only modification of the standard RK approximation. Stabilization using IG-RKPM is thus very straightforward compared to the explicit version, can be added to existing codes easily, and introduces virtually no additional cost. This is in contrast to explicit differentiation, which requires considerable more computational expense and implementation effort.

An important component of meshfree formulations is the selection of domain integration. For Gaussian integration, high order rules are necessary in order to ensure solution accuracy, while nodal integration yields poor accuracy and is unstable without special treatment [20, 21]. Herein we employ higher order SCNI [22, 23] which provides accurate and stable solutions and avoids the need of expensive high order quadrature.

Table 1 Implicit gradient RKPM vector.

Method	$\mathbf{H}_{\alpha}^{\mathrm{T}}$
SU/PG [1]	$[1, \ -\tau a_1, -\tau a_2, 0, \ \ldots \ , \ 0]$
G/LS [2]	$[1, \ -\tau a_1, -\tau a_2, -2\tau k, -2\tau k, 0, \ \ldots \ , \ 0]$
SGS [3]	$[1, \ -\tau a_1, -\tau a_2, 2\tau k, 2\tau k, \ 0, \ldots \ , \ 0]$

3.3 Selection of the Stabilization Parameter

The selection of the stabilization parameter was traditionally based on obtaining the exact solution at nodes in the one-dimensional Dirichlet problem of (1) in the absence of a source term [1]. The exact solution for this particular case is

$$u^e(x) = C_1 + C_2 e^{ax/k} \tag{21}$$

where C_1 and C_2 depend on the prescribed boundary conditions. Consider the trial and test functions approximated by

$$\begin{aligned} u^h &= \sum_{I=1}^{NP} \Psi_I u_I, \\ \tilde{v}^h &= \sum_{I=1}^{NP} \tilde{\Psi}_I u_I, \end{aligned} \tag{22}$$

where $\{\Psi_I\}_{I=1}^{NP}$ is the set of standard trail shape functions, e.g., finite element or RK approximations, $\left\{\tilde{\Psi}_I\right\}_{I=1}^{NP}$ is the set of corresponding stabilized test shape functions, and NP is the number of approximation functions.

Substitution of (22) into (11) yields

$$\sum_{J=1}^{NP} B\left(\tilde{\Psi}_I, \Psi_J\right) u_J = 0, \quad \forall I. \tag{23}$$

Due to the lack of Kronecker delta property in the RKPM shape functions, the relationship between the generalized coordinates u_I^e and the exact nodal values $\widehat{u}_I^e \equiv u^e\left(x_I\right) = A + Be^{ax_I/k}$ must be considered:

$$u_I^e = \sum_{J=1}^{NP} {\Lambda_{IJ}}^{-1} \widehat{u}_I^e \tag{24}$$

where $\Lambda_{IJ} = \Psi_J\left(x_I\right)$. Note that for linear finite elements, $\Lambda_{IJ} = \delta_{IJ}$. Substitution of the above into (23), and considering the partition of unity in the trial functions, the constants associated with the boundary conditions disappear:

$$\sum_{J=1}^{NP} \left\{ \int_\Omega k \tilde{\Psi}_{I,x} \Psi_{J,x} \mathrm{d}\Omega + \int_\Omega a \tilde{\Psi}_I \Psi_{J,x} \mathrm{d}\Omega \right\} E_J = 0, \qquad \forall I \tag{25}$$

where $E_I = \sum_{J=1}^{NP} \Lambda_{IJ}{}^{-1} e^{ax_J/k}$. Using a stabilized shape function with nodal stabilization parameter τ_I:

$$\tilde{\Psi}_I = \Psi_I + \tau_I \mathbb{L}\Psi_I \tag{26}$$

we have, picking row I in (25):

$$\tau_I = -\frac{\int_\Omega k\Psi_{I,x}\overline{E}\mathrm{d}\Omega + \int_\Omega a\Psi_I\overline{E}\mathrm{d}\Omega}{\int_\Omega k\{\mathbb{L}\Psi_I\}_{,x}\overline{E}\mathrm{d}\Omega + \int_\Omega a\mathbb{L}\Psi_I\overline{E}\mathrm{d}\Omega} \tag{27}$$

where $\overline{E}_I(x) = \sum_{J=1}^{NP} \Psi_{J,x}E_J$. For linear finite element methods in uniform discretizations, the above equation is not a function of nodal index, and yields the classical stability parameter for SU/PG [1]:

$$\tau = \frac{h}{2a}\left(\coth\left(Pe_h\right) - \frac{1}{Pe_h}\right). \tag{28}$$

In [11] it has been discussed that for RKPM, parameters in the form of (27) depend on the approximation functions on the global level due to the transformation between generalized values u_I and nodal values $u^h(x_I)$ and cannot be simplified to a form such as (28). Thus, the generalization of the condition (27) for higher spatial dimensions is not straightforward. Herein, we employ the classical parameter (28) which is often generalized to higher spatial dimensions as [1]:

$$\tau = \frac{h}{2a}\left(\coth\left(Pe_{h,a}\right) - \frac{1}{Pe_{h,a}}\right) \tag{29}$$

where $Pe_{h,a} = \|\mathbf{a}\| h_a/2k$, and h_a is the grid (or element) dimension along the direction of advection. For RKPM, the spacing h_a may be taken as the length of a representative nodal domain in the direction of the advection. The parameter (29) has been shown to be suitable for RKPM with linear basis, so long as the support parameter is not larger than roughly three times the nodal spacing [11].

4 Numerical Examples

In all numerical examples, RK approximations with linear basis and quartic B-spline kernels with a normalized support of two are employed. In this case, all stabilization methods with implicit gradients are identical due to the order of the basis vector

used. In the comparisons made, "RKPM" denotes RKPM with no stabilization, "SU/PG RKPM" denotes RKPM with standard (explicit) SU/PG stabilization, and "IG-RKPM" denotes implicit gradient RKPM. For domain integration, high order SCNI [20] is employed with 2^{nd} order Gaussian quadrature in each nodal cell.

4.1 One-dimensional Model Problem

Consider the one-dimensional homogenous version of the model problem (1) on a unit domain with $a/k = 200.0$, and $s = 1.0$, giving a grid Péclet number of 5.0 with 21 nodes employed. RKPM, RKPM with SU/PG stabilization, and IG-RKPM are compared in Fig. 1. RKPM without stabilization yields large spurious oscillations in the solution. The two stabilized methods give solutions which agree with the exact solution, and very little difference between the two is observed, indicating that a large increase in efficiency can be obtained with little lost by employing implicit stabilization.

4.2 Advection Skew to the Discretization with Outflow Boundary

Here a two-dimensional Dirichlet version of (1) with advection skew to the discretization is considered, as shown in Fig. 2, where the jump in inflow boundary condition along $x = 0.0$ is located at $y = 0.2$. A characteristic of this problem is that both internal layers and boundary layers exist in the solution. The boundary layers cause difficulty for numerical methods, just as in the one-dimensional case. Constant advection and isotropic diffusion parameters are chosen as $\mathbf{a} = (\cos\ \theta,\ \sin\ \theta)$ and $k = 10^{-6}$, respectively, and the domain is taken to be $[0.0, 1.0] \times [0.0, 1.0]$ so that the flow is convection-dominated. The domain is discretized by 31×31 nodes, which gives a grid Péclet number much larger than unity.

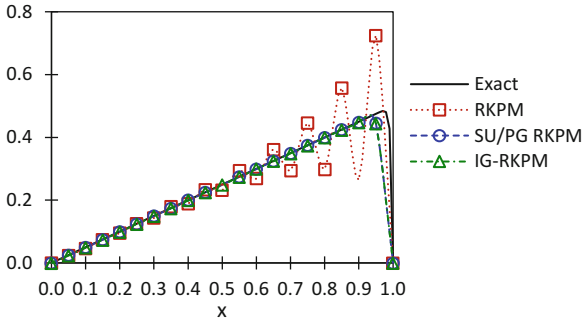

Fig. 1 Comparison between RKPM, explicit SU/PG, and IG-RKPM in the model problem. Markers indicate the solution at nodal locations.

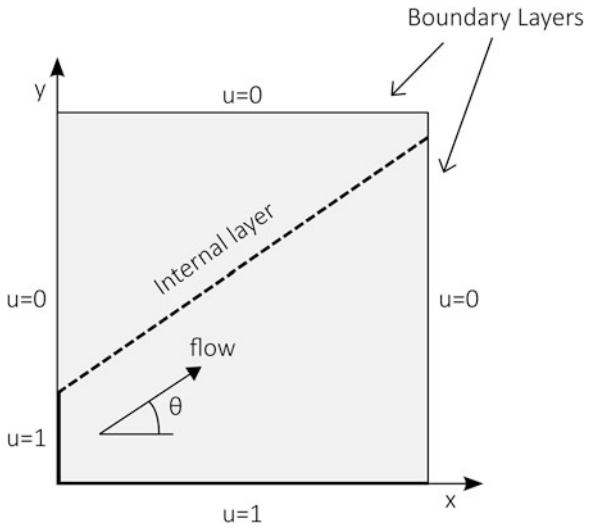

Fig. 2 Problem statement for advection skew to the discretization.

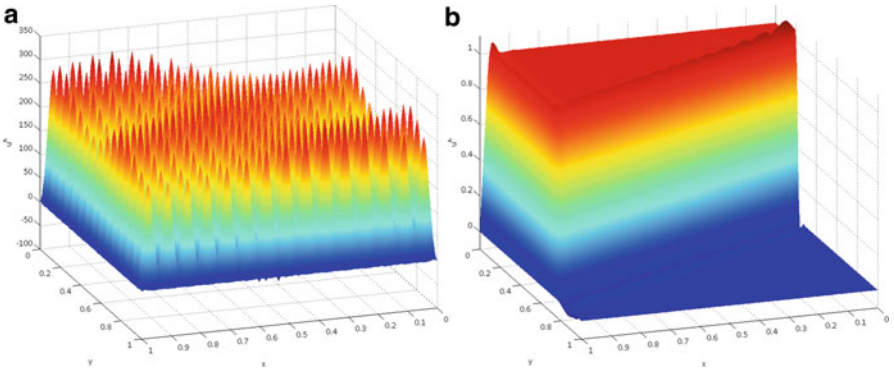

Fig. 3 Advection skew to the discretization with $\theta = \text{atan}(0.5)$ for (a) RKPM, and (b) IG-RKPM.

First, the case of $\theta = \text{atan}(0.5)$ is considered, with RKPM and IG-RKPM employed. As seen in Fig. 3, the magnitude of the RKPM solution is several orders of magnitude greater than the exact solution (essentially pure advection of the boundary condition), while IG-RKPM gives a stable solution. The values of $\theta = \text{atan}(1.0)$ and $\theta = \text{atan}(2.0)$ are then considered with IG-RKPM, where the method exhibits stability in the presence of the fine boundary layers as shown in Fig. 4. The slight overshoots in the solution are expected in linear methods which do not have the variation diminishing property.

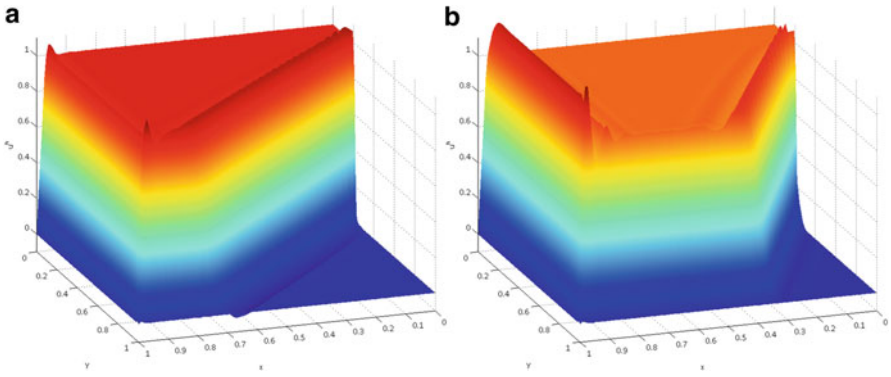

Fig. 4 Advection skew to the discretization with IG-RKPM for (a) $\theta = \text{atan}(1.0)$, and (b) $\theta = \text{atan}(2.0)$.

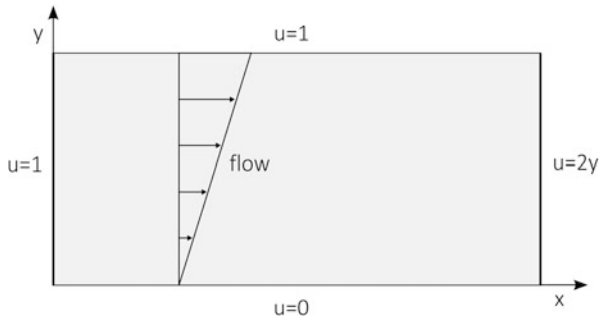

Fig. 5 Thermal boundary layer problem statement.

4.3 Thermal Boundary Layer Problem

Consider the problem statement shown in Fig. 5 with linearly distributed advection $\mathbf{a} = (2.0y,\ 0.0)$, and diffusivity $k = 7.0 \cdot 10^{-4}$. The domain is taken as $[0.0, 1.0] \times [0.0, 0.5]$ and is discretized by 31×16 nodes. This problem can be interpreted as one exhibiting a thermal boundary layer on a steady flow between two plates, where the top plate has unit velocity and the bottom plate is fixed. The grid Péclet number calculated from the advection speed at the top surface of the domain and the chosen nodal spacing is larger than unity. The RKPM and IG-RKPM methods are considered, with the results shown in Fig. 6. Again, RKPM gives an oscillatory solution while IG-RKPM gives a stable solution.

5 Conclusion

Meshfree methods offer smooth approximation spaces suitable for the gradient-type stabilization employed for convection-dominated problems. While for linear finite elements, all of the standard stabilization methods coincide due to vanishing higher

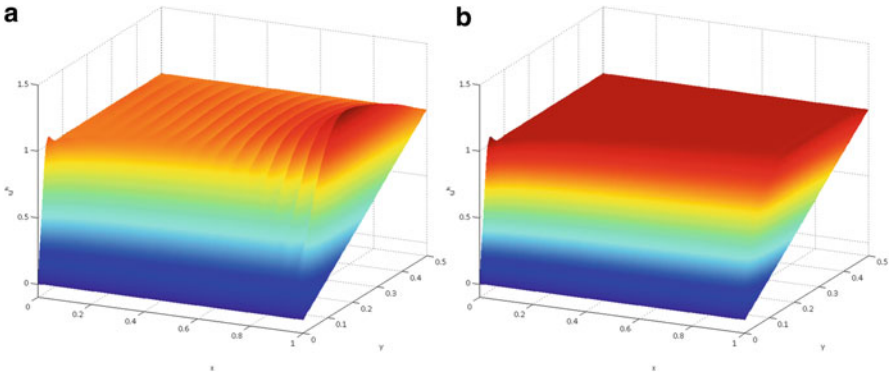

Fig. 6 Solutions for the thermal boundary layer problem for (a) RKPM and (b) IG-RKPM.

order derivatives on element interiors, these methods can be properly constructed by the RK approximation using linear basis. Gradient terms necessary, however, are computationally expensive, due to the moment matrix inversion involved in the gradients of meshfree shape functions. This problem is particularly exacerbated in the G/LS and SGS methods where third order derivatives appear in the weak form of the problem.

In this work, a new approach to construct a stable RKPM method for convection-dominated problems is presented. Terms for the gradient-type stabilized methods are implicitly introduced into the reproducing conditions under a unified framework that can include the SU/PG, G/LS, and SGS methods. The implicit gradients completely circumvent the costly derivatives otherwise necessary for stabilization. The only deviation from the standard RKPM method is the modification of the constant vector in the RK approximation for the test functions, and thus virtually no additional computational cost is introduced, and implementation is simple. The benchmark problems tested showed good performance of the proposed method and agreement with solutions by explicit stabilization.

Acknowledgements The support of this work by US Army Engineer Research and Development Center under contract W912HZ-07-C-0019 is greatly acknowledged.

References

1. Brooks, A.N., Hughes, T.J.R.: Streamline upwind/Petrov-Galerkin formulations for convection dominated flows with particular emphasis on the incompressible Navier-Stokes equations. Comput. Methods Appl. Mech. Eng. **32**, 199–259 (1982)
2. Hughes, T.J.R., Franca, L.P., Hulbert, G.M.: A new finite element formulation for computational fluid dynamics: VIII. The Galerkin/least-squares method for advective-diffusive equations. Comput. Methods Appl. Mech. Eng. **73**, 173–189 (1989)

3. Franca, L.P., Frey, S.L., Hughes, T.J.R.: Stabilized finite element methods: I. Application to the advective-diffusive model. Comput. Methods Appl. Mech. Eng. **95**, 253–276 (1992)
4. Johnson, C., Nävert, U., Pitkäranta, J.: Finite element methods for linear hyperbolic problems. Comput. Methods Appl. Mech. Eng. **45**, 285–312 (1984)
5. Hughes, T.J.R.: Multiscale phenomena: Green's functions, the Dirichlet-to-Neumann formulation, subgrid scale models, bubbles and the origins of stabilized methods. Comput. Methods Appl. Mech. Eng. **127**, 387–401 (1995)
6. Hughes, T.J.R., Feijóo, G.R., Mazzei, L., Quincy, J.B.: The variational multiscale method—a paradigm for computational mechanics. Comput. Methods Appl. Mech. Eng. **166**, 3–24 (1998)
7. Franca, L.P., Farhat, C.: Bubble functions prompt unusual stabilized finite element methods. Comput. Methods Appl. Mech. Eng. **123**, 299–308 (1995)
8. Brezzi, F., Bristeau, M.O., Franca, L.P., Mallet, M., Rogé, G.: A relationship between stabilized finite element methods and the Galerkin method with bubble functions. Comput. Methods Appl. Mech. Eng. **96**, 117–129 (1992)
9. Baiocchi, C., Brezzi, F., Franca, L.P.: Virtual bubbles and Galerkin-least-squares type methods (Ga. LS). Comput. Methods Appl. Mech. Eng. **105**, 125–141 (1993)
10. Günther, F., Liu, W.K., Diachin, D., Christon, M.A.: Multi-scale meshfree parallel computations for viscous, compressible flows. Comput. Methods Appl. Mech. Eng. **190**, 279–303 (2000)
11. Fries, T.P., Matthies, H.G.: A stabilized and coupled meshfree/meshbased method for the incompressible Navier–Stokes equations—part I: Stabilization. Comput. Methods Appl. Mech. Eng. **195**, 6205–6224 (2006)
12. Fries, T.P., Matthies, H.G.: A stabilized and coupled meshfree/meshbased method for the incompressible Navier–Stokes equations—Part II: Coupling. Comput. Methods Appl. Mech. Eng. **195**, 6191–6204 (2006)
13. Huerta, A., Fernández-Méndez, S.: Time accurate consistently stabilized mesh-free methods for convection dominated problems. Int. J. Numer. Methods Eng. **56**, 1225–1242 (2003)
14. Chi, S.W., Chen, J.S., Hu, H.Y., Yang, J.P.: A gradient reproducing kernel collocation method for boundary value problems. Int. J. Numer. Methods Eng. **93**, 1381–1402 (2013)
15. Li, S., Liu, W.K.: Reproducing kernel hierarchical partition of unity. Part I: Formulation and theory. Int. J. Numer. Methods Eng. **45**, 251–288 (1999)
16. Li, S., Liu, W.K.: Reproducing kernel hierarchical partition of unity. Part II: Applications. Int. J. Numer. Methods Eng. **45**, 289–317 (1999)
17. Chen, J.S., Zhang, X., Belytschko, T.: An implicit gradient model by a reproducing kernel strain regularization in strain localization problems. Comput. Methods Appl. Mech. Eng. **193**, 2827–2844 (2004)
18. Liu, W.K., Jun, S., Zhang, Y.F.: Reproducing kernel particle methods. Int. J. Numer. Methods Fluids **20**, 1081–1106 (1995)
19. Chen, J.S., Pan, C., Wu, C.T., Liu, W.K.: Reproducing kernel particle methods for large deformation analysis of nonlinear structures. Comput. Methods Appl. Mech. Eng. **139**, 195–227 (1996)
20. Dolbow, J., Belytschko, T.: Numerical integration of the Galerkin weak form in meshfree methods. Comput. Mech. **23**, 219–230 (1999)
21. Beissel, S., Belytschko, T.: Nodal integration of the element-free Galerkin method. Comput. Methods Appl. Mech. Eng. **139**, 49–74 (1996)
22. Chen, J.S., Wu, C.T., Yoon, S., You, Y.: A stabilized conforming nodal integration for Galerkin mesh-fee methods. Int. J. Numer. Methods Eng. **50**, 435–466 (2001)
23. Chen, J.S., Hu, W., Puso, M.: Orbital HP-clouds for solving Schrödinger equation in quantum mechanics. Comput. Methods Appl. Mech. Eng. **196**, 3693–3705 (2007)